DOI: 10.1002/cplu.201300428

2,6-Bis(arylsulfonyl)anilines as Fluorescent Scaffolds through Intramolecular Hydrogen Bonds: Solid-State Fluorescence Materials and Turn-On-Type Probes Based on Aggregation-Induced Emission

Teruo Beppu, So Kawata, Naoya Aizawa, Yong-Jin Pu, Yasuyuki Abe,* Yoshihiro Ohba, and Hiroshi Katagiri*[a]

A series of 2,6-bis[aryl(alkyl)sulfonyl]anilines were synthesized by nucleophilic aromatic substitution of 2,6-dichloronitrobenzene with various aryl or alkyl thiolates (benzyl-, phenyl-, 2-naphthyl-, and 2-aminophenyl thiolate), followed by hydrogenation and subsequent oxidation. All prepared 2,6-bis-[aryl-(alkyl)sulfonyl]anilines showed high fluorescence emissions in the solid state; X-ray structures revealed well-defined intramolecular hydrogen bonds, which served to immobilize the rotatable amino group and generate a fluorescence enhancement in addition to improved photostability. Moreover, absorption and fluorescence spectra showed redshifts in the order of benzyl < phenyl < 2-naphthyl in solution and the solid state, and DFT calculations confirmed charge transfer from the central aniline unit to the side aryl groups through the sulfonyl bridges, which together indicated the push–pull effect with an extended π-conjugated system comprising the 2,6-bis(arylsulfonyl)aniline unit. Furthermore, 2,6-bis(2-aminophenylsulfonyl)aniline, with rotatable amino groups at the flanking aryl units, was affected by fluorescence quenching in solution. This nonemissive state showed an enhanced environmental sensitivity to solvent polarity and viscosity, along with a "turn-on" fluorescence response in frozen solvent and in the aggregated form. 2,6-Bis(2-aminophenylsulfonyl)aniline behaved as a turn-on fluorescence probe for selective detection of DNA based on its aggregation-induced emission.

Introduction

Organic luminophores have been widely studied for decades and have been used in a variety of applications in which luminescence is desired.[1,2] In particular, although organic luminescence has been extensively studied in solution for luminophores in the monomeric form, the search for materials for solid-state emissions has increased in importance for various optoelectronic applications, such as organic light-emitting diodes (OLEDs)[3] and dye lasers.[4,5] Aggregation-induced emission (AIE) has been recently utilized in advanced applications by using the concept of a "turn-on" luminescence response in chemosensors and bioprobes.[6] The underlying principle for the observation of most organic luminophores in dilute conditions is based on a molecular design that employs a flat and rigid framework for effective extension of the π-conjugation system. The π stacking of molecules at high concentrations and in the solid state leads to subsequent quenching and lowered photosensitivity through intermolecular energy-transfer processes;[7] a phenomenon widely known as "concentration quenching," which imposes limits on the effective application of fluorescent probes and electroluminescent devices. In response to this problem, the use of a bulky group or twisted molecular geometry has been recently introduced to prevent the intermolecular stacking of luminophores and generate a solid-state emission.[8] This concept relies on the presence of twisted rotatable bonds; in solution, free bond rotation renders the molecules nonemissive, whereas immobilization of the relevant bonds in aggregation gives rise to emissive properties, which produce desirable phenomena, such as a turn-on type of probe response.[6a,9,10] Therefore, unsurprisingly, the design and synthesis of conceptually new scaffolds for solid-state luminescence materials is a central research topic in chemistry and materials science.

We report herein the preparation of 2,6-bis(arylsulfonyl)aniline (BArSA) as a novel scaffold for luminophores (Scheme 1). The concept of the molecular design includes the following two unique points for enhancement of the fluorescence properties: 1) barriers to rotation of amino groups are accomplished through intramolecular hydrogen-bonds motifs, and 2) amino and sulfonyl moieties are employed to improve fluorescence through enhanced push–pull and π-conjugation ef-

[a] T. Beppu, S. Kawata, N. Aizawa, Prof. Dr. Y.-J. Pu, Prof. Dr. Y. Abe, Prof. Dr. Y. Ohba, Prof. Dr. H. Katagiri
Graduate School of Science and Engineering
Yamagata University, 4-3-16 Jonan, Yonezawa
Yamagata 992-8510 (Japan)
Fax: (+81) 238-26-3743
E-mail: y-abe@yz.yamagata-u.ac.jp
kgri7078@yz.yamagata-u.ac.jp

Supporting information for this article is available on the WWW under http://dx.doi.org/10.1002/cplu.201300428. It contains ^{1}H and ^{13}C NMR spectroscopy data, HRMS data for all new compounds, UV/Vis and fluorescence spectra, MO calculation details, powder XRD data, and X-ray crystallographic data and crystallographic files.

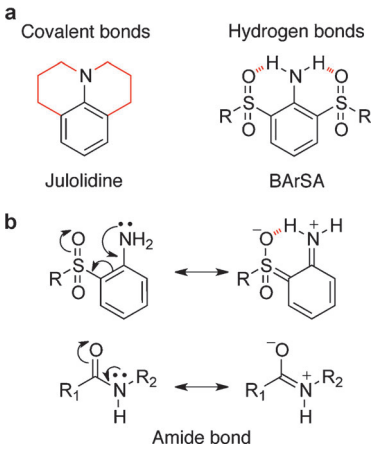

Scheme 1. Schematic representation of the BArSAs: a) a comparison of the structural properties between julolidine and BArSAs, and b) the similarity in resonance forms between the arylsulfonyl moiety and the amide bond.

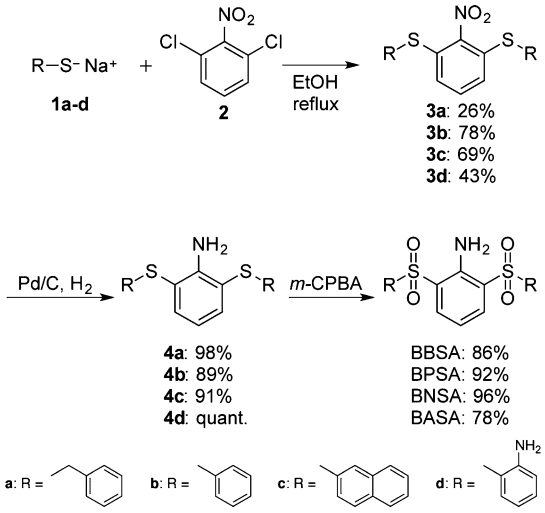

Scheme 2. Synthetic route to BArSA derivatives.

fects. On the first point, although the presence of an amino group strongly increases the HOMO level of π-conjugated molecules by an electron-donating effect, the freely rotating C–N bond is not conducive to fluorescence owing to vibrational quenching. This problem is addressed by employing a julolidine framework, in which the amino group is made rigid by covalent bonds; a strategy that has been widely used in fluorescent architectures (e.g., Texas Red) to increase quantum yields and enhance stabilities (Scheme 1a).[11] In contrast, the amino group of BArSA is rigidified by intramolecular hydrogen bonds in a similar manner to the structural immobilization of julolidine, which is schematically represented in comparison to the conjugation system of an amide bond in Scheme 1b. On the second point, push–pull systems have also been applied to a variety of luminophores because of marked increases in observed molar extinction coefficients and longer wavelengths.[12] The amino and sulfonyl groups of BArSAs would function as strong electron donors and acceptors, respectively, to allow the creation of an effective push–pull system.

Results and Discussion

Synthesis of BArSAs

All BArSA derivatives discussed herein, including 2,6-bis(phenylsulfonyl)aniline (BPSA), 2,6-bis(2-naphthylsulfonyl)aniline (BNSA), 2,6-bis(2-aminophenylsulfonyl)aniline (BASA), and alkyl derivative 2,6-bis(2-benzylsulfonyl)aniline (BBSA) were synthesized by the nucleophilic aromatic substitution of 2,6-dichloronitrobenzene (**2**) with the corresponding aryl (or benzyl) thiolates (**1a–d**), followed by palladium-catalyzed hydrogenation (to **4**), and subsequent oxidation with *meta*-chloroperoxybenzoic acid (*m*-CPBA; Scheme 2). All new compounds were characterized by ^{1}H and ^{13}C NMR spectroscopy and HRMS (see the Supporting Information). Moreover, elemental analyses and single-crystal X-ray structure determinations were performed for **4b** and all BArSAs.

Validation of intramolecular hydrogen-bond formation

The presence of intramolecular hydrogen bonds, which are the key component theorized to stabilize the amino groups on BArSAs, was established by comparison of the structural properties of BPSA and sulfide precursor **4b**. In the crystal structures shown in Figure 1a, typical intramolecular hydrogen

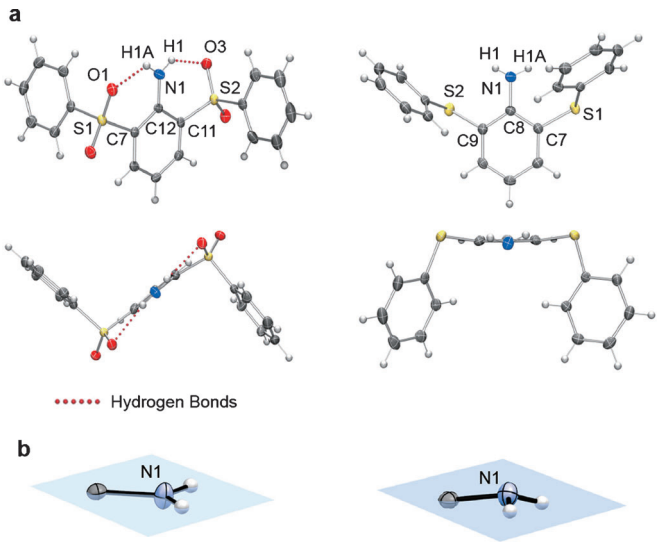

Figure 1. Crystal structures of BPSA (left) and **4b** (right): a) ORTEP drawing of the side and top views with thermal ellipsoids at 50% probability, and b) partial view focused on the amino groups and orbital hybridization at nitrogen atoms.

bonds were observed between the amino and sulfonyl groups of BPSA; the obtained parameters indicate that these hydrogen bonds were especially strong: N1···O3 = 2.826(2) Å, N1–H1 = 0.85(2) Å, H1···O3 = 2.15(2) Å, and N1–H1···O3 = 136(2)°; N1···O1 = 2.806(2) Å, N1–H1A = 0.86(2) Å, H1A···O1 = 2.14(2) Å, and N1–H1A···O1 = 134(2)°. Moreover, the geometry around the amino group of BPSA was clearly in the sp^2 configuration,

Table 1. Crystallographically determined bond lengths, ^{1}H NMR chemical shifts, and IR absorption frequencies of BPSA and **4b**.

	N–C [Å]	S–C [Å]	C–C [Å]	δ_{NH} [ppm][a]	ν_{NH} [cm^{-1}][b]
BPSA	1.346(2)	1.761(2) [S1–C7] 1.761(2) [S2–C11]	1.421(2) [C12–C7] 1.423(2) [C12–C11]	6.77	3469, 3367
4b	1.380(2)	1.775(2) [S1–C7] 1.773(2) [S2–C9]	1.412(2) [C8–C7] 1.419(2) [C8–C9]	4.98	3469, 3363

[a] Measured in $CDCl_3$ at 35 °C. [b] Measured in KBr matrix.

whereas that of **4b** was sp^3 geometry, as shown in Figure 1b (mean plane (C12, H1, H1A)···N1 = 0.018(13) Å in BPSA, and mean plane (C8, H1, H1A)···N1 = 0.221(9) Å in **4b**). The C–N distance in BPSA was shorter than that in **4b**, whereas the S–C bonds were shorter and aromatic C–C bonds were elongated (Table 1). Finally, the appearance of an amine chemical shift (δ_{NH}) in the ^{1}H NMR spectrum of BPSA at δ = 6.77 ppm showed characteristics of an amide functionality (Figure S20 in the Supporting Information), whereas in **4b** the analogous signal observed at δ = 4.98 ppm corresponded to an ordinary aromatic amine (Figure S12 in the Supporting Information). Analysis of IR absorption spectra provided further evidence for hydrogen-bond formation; the absorption band corresponding to the amino group of BPSA was observed at a lower frequency than that of **4b**. Thus, all parameters noted in Table 1 are suggestive of intramolecular hydrogen bonds, as shown in Scheme 1.

Absorbance and fluorescence properties of BBSA, BPSA, and BNSA

BBSA, BPSA, and BNSA exhibited efficient emissions from λ = 393–406 nm with high quantum yields in acetonitrile (Table 2 and Figure 2a).[13] With respect to the optical properties of BPSA, it should be noted that the wavelength of maximum absorbance (λ^{max}_{abs}) showed a redshift of 20 nm relative to sulfide precursor **4b**, and the molar extinction coefficient (ε_{max}) was 17% higher than that of **4b**; this is indicative of the construction of an effective push–pull system between amino and sulfonyl groups. As another special feature of the BArSAs, both absorption and fluorescence spectra exhibited a redshift relative to the extent of π conjugation, for example, BBSA < BPSA < BNSA (Figure 2a). Values of λ^{max}_{abs} and λ^{max}_{em} were higher for BArSA derivatives than those of the respective benzyl, phenyl, and 2-naphthyl sulfide precursors (**4a**,**b**,**c**) themselves. Therefore, these redshifts can be ascribed to the bis-arylsulfonyl unit; thus, the BArSAs appeared to possess a flexible π-conjugation system.[14] As previously mentioned, luminophores constructed based on the rigid flat design are commonly nonemissive in the solid state. In contrast, BBSA, BPSA, and BNSA showed solid-state emissions in the powder form, with quantum yields of Φ = 0.31, 0.36, and 0.28, respectively (Table 2 and Figure 2b). The λ^{max}_{abs} of BBSA, BPSA, and BNSA in solid-state exhibited

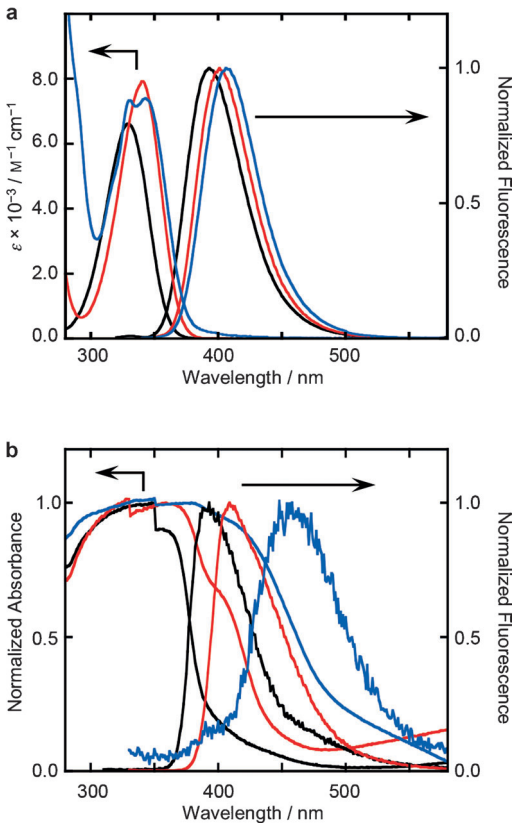

Figure 2. a) Absorption and fluorescence spectra of BBSA (black), BPSA (red), and BNSA (blue) in acetonitrile; b) solid-state absorption and fluorescence spectra. Absorption spectra were measured by using the reflection method in an integrating sphere with lamp-switching wavelengths of 330 (BPSA, BNSA) or 350 nm (BBSA).

Table 2. Absorption and luminescence properties of **4b**, BBSA, BPSA, and BNSA.[a]

	Solution [acetonitrile]				Solid state [powder]		
	λ^{max}_{abs} [nm]	ε_{max} [M^{-1}cm^{-1}]	λ^{max}_{em} [nm][b]	Φ[c]	λ^{max}_{abs} [nm][d]	λ^{max}_{em} [nm][e]	Φ[f]
4b	322	6800	383	0.049	316	387	0.030
BBSA	329	6600	393	0.50	348	393	0.31
BPSA	340	7900	401	0.37	359	409	0.36
BNSA	343	7400	406	0.31	379	458	0.28

[a] UV/Vis spectra recorded at 5.0×10^{-5} M for **4b** and BArSAs; fluorescence spectra recorded at 2.5×10^{-5} M for **4b** and 5.0×10^{-6} M for BBSA, BPSA, and BNSA. [b] Excitation at λ = 300 (**4b**, BBSA) and 320 nm (BPSA, BNSA). [c] Determined relative to anthracene in benzene (Φ = 0.29). [d] Reflection spectra in an integrating sphere. [e] Excitation at λ = 300 (**4b**, BBSA) and 320 nm (BPSA, BNSA). [f] Determined in an integrating sphere.

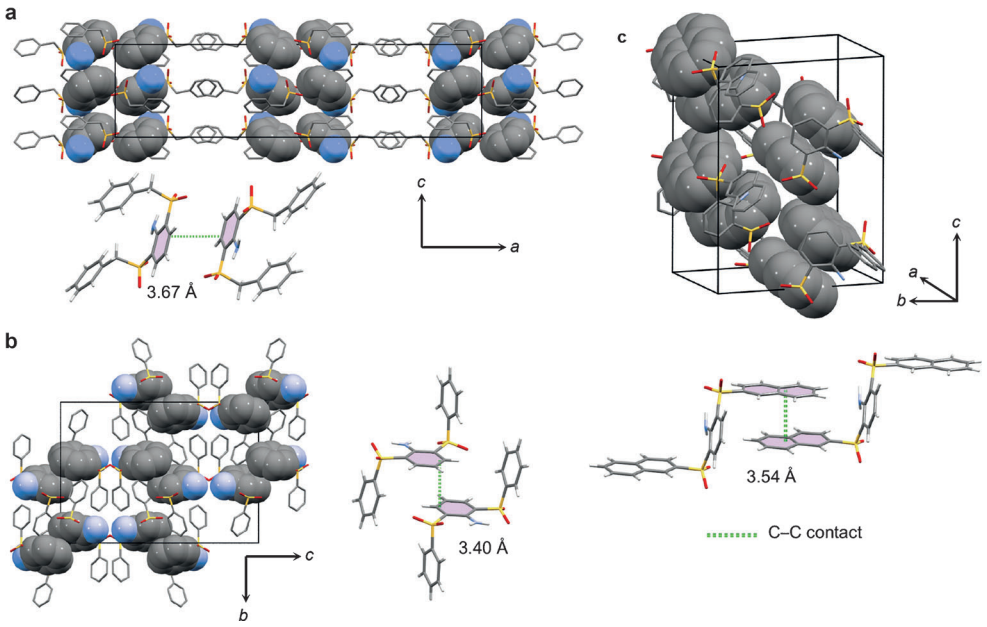

Figure 3. Crystal structures of a) BBSA, b) BPSA, and c) BNSA. Dimerized aromatics are illustrated as space-filling models and as partially cutaway views with distances of interatomic C–C contacts.

redshifts of 19, 19, and 36 nm, respectively, compared with those in solution. In addition, the λ^{max}_{em} values of BPSA and BNSA were observed at longer wavelengths than those observed in solution (8 and 52 nm, respectively). These results indicate the presence of an intermolecular interaction between the aromatic moieties of BBSA, BPSA, and BNSA. Specifically, the central sulfonylaniline units of BBSA and BPSA participated in dimeric structure formation (Figure 3a and b), and the naphthyl moieties of BNSA took part in π stacking in its dimer form (Figure 3c). The dimerized aromatic rings adopted an antiparallel formation with distances within the acceptable range of π–π stacking interactions; the closest distances between carbon atoms were 3.67(7), 3.40(0), and 3.54(4) Å in BBSA, BPSA, and BNSA, respectively. The long wavelength of solid-state absorption spectra in these BArSAs were thus attributed to a J-dimer form;[7b,15] the bent shape of BArSAs is advantageous to solid-state emission, which is quite different from ordinary rigid, flat luminophores. To confirm the flexibility of the π-conjugation system present in BArSAs, DFT calculations were performed on BPSA and **4b** at the B3LYP/6-31G(d) level. Optimizations were performed by using the respective crystal structures as the initial geometries; the resulting conformations for both compounds were in a good agreement with those of the crystal structures. As shown in Figure 4, the HOMO of BPSA is located at the central aniline unit and the LUMO extends through the sulfonyl groups to the edge phenyl rings. On the other hand, in **4b**, the HOMO and LUMO are mainly located at the central aniline unit. These results indicate that the BArSA framework demonstrates charge transfer from aniline to the phenyl rings through the sulfonyl bridges. Both the HOMO and LUMO energy levels of BPSA were lower than those of **4b**; this is assumed to arise because of the strong electron-withdrawing effect of the sulfonyl groups. More importantly, the HOMO–

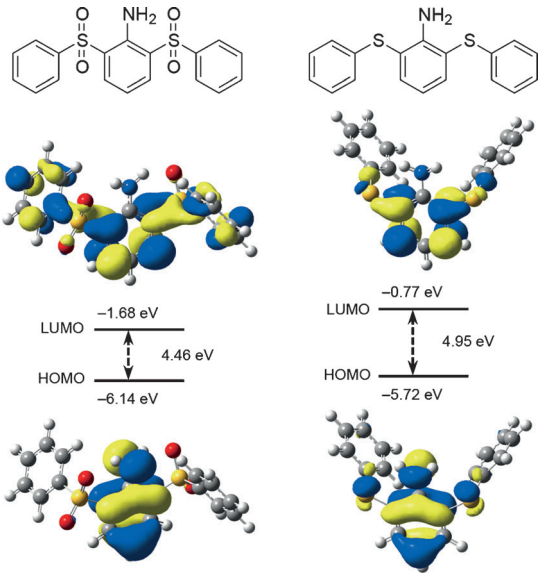

Figure 4. HOMO and LUMO orbital representations for BPSA (left) and **4b** (right).

LUMO energy gap of BPSA showed a clear decrease from that of **4b**; this clearly indicates the construction of an effective push–pull and π-conjugation system.

Fluorescence properties of BASA

The solid-state fluorescence properties of BArSAs prompted us to explore an additional molecular framework, namely, the introduction of amino groups in the form of a BArSA skeleton to diminish fluorescence by using the rotatable amino moieties.

Table 3. Absorption and emission properties of BASA in selected solvents.[a]

Solvent	λ^{max}_{abs} [nm]	λ^{max}_{em} [nm][b]	ε [M^{-1} cm^{-1}]	Φ[c]
THF	345	432	12400	0.0080
1-BuOH	343	450	13300	0.0056
2-PrOH	341	454	12200	0.0053
1-PrOH	343	457	12100	0.0050
EtOH	342	456	11300	0.0029
CH_3CN	341	473	12500	0.0019
CH_3OH	341	468	12300	0.0018
DMF	348	478	12800	0.0027
DMSO	350	491	13300	0.0020
powder	339[d]	396	–	0.15[e]

[a] UV/Vis spectra recorded at 5.0×10^{-5} M; fluorescence spectra recorded at 2.5×10^{-5} M. [b] Excitation at $\lambda=340$ nm. [c] Determined relative to anthracene in benzene. [d] Reflection spectra in an integrating sphere. [e] Determined in an integrating sphere.

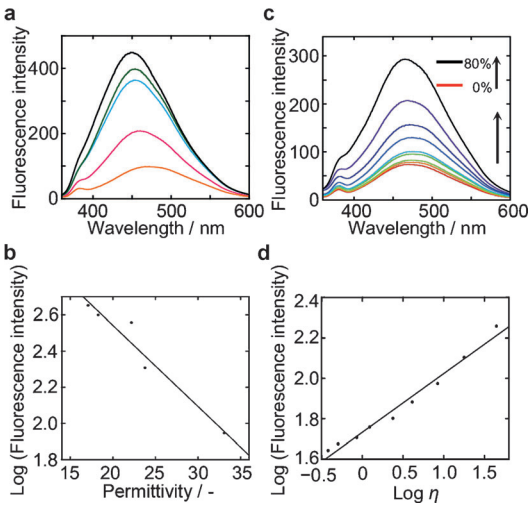

Figure 5. Fluorescence spectra of BASA: a) fluorescence spectra of BASA in 1-BuOH (black), 2-PrOH (green), 1-PrOH (light blue), EtOH (pink), and CH_3OH (orange); b) plot of fluorescence intensity at $\lambda=450$ nm versus solution permittivity; c) fluorescence spectra of BASA in CH_3CN–PEG1000 (PEG = polyethylene glycol) mixtures measured with different weight fractions of PEG1000: 0 (red), 10 (orange), 20 (yellow green), 30 (light green) 40 (light blue), 50 (cyan), 60 (blue), 70 (purple), 80 wt% (black); and d) plot of fluorescence intensity at $\lambda=464$ nm versus solution viscosity.

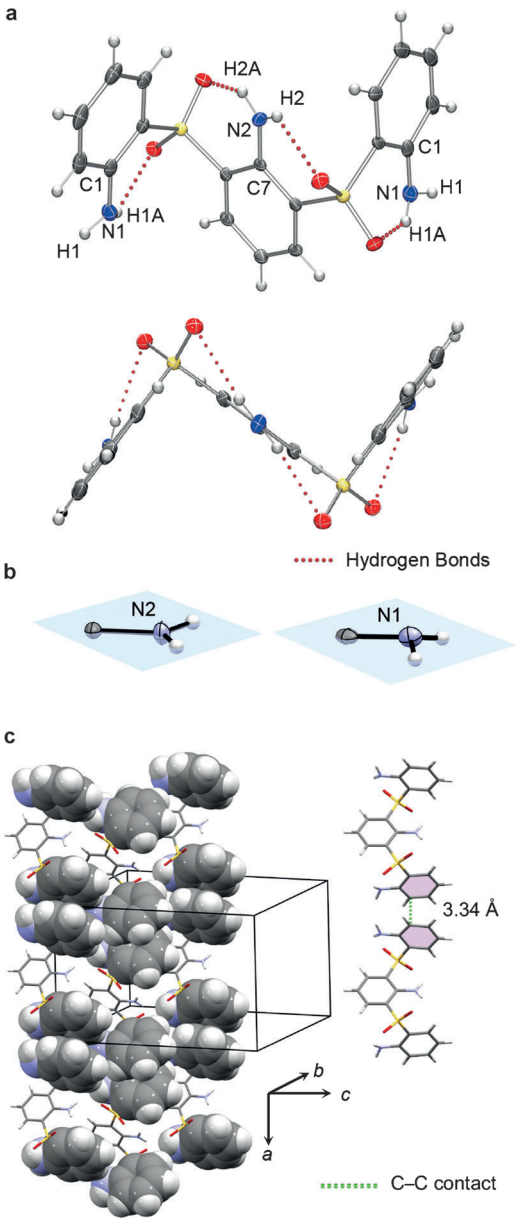

Figure 6. Crystal structures of BASA: a) ORTEP drawing of the side and top views with thermal ellipsoids at 50% probability, b) partial view focused on the amino groups and orbital hybridization at nitrogen atoms, and c) packing structure with dimerized aromatics illustrated as space-filling models and with partially cutaway views of an interatomic C–C contact.

This strategy is based on a weak fluorescence originating from the twisted intramolecular charge-transfer (TICT) states, which is not an unusual phenomenon for rotatable amino groups.[16] Thus, we thought that, if the nonemissive state could be switched to an emissive state, turn-on-type probes would be observed. BASA demonstrated low quantum yields in a variety of common solvents (Table 3); the value of Φ was two orders of magnitude lower than that of BPSA in acetonitrile ($\Phi=$ 0.0019 and 0.37 for BASA and BPSA, respectively). In addition, BASA showed solvatochromic fluorescence and the value of redshifts were observed to increase with increasing solvent polarity (e.g., $\lambda^{max}_{em}=432$ and 491 nm in THF and in DMSO, respectively; Table 3 and Figure S44e in the Supporting Information); a significant correlation between solvent permittivity and fluorescence intensity was found among the various alcohols examined ($R^2=0.95$; Figure 5a and b). The emission intensity of BASA also increased in viscous solvents prepared from acetonitrile–PEG mixtures (Figure 5c),[17] with significant correlation between solvent viscosity and fluorescent intensity ($R^2=$ 0.98; Figure 5d). It should be noted that the resulting higher emission intensities in nonpolar and viscous solvents are particularly seen in molecular rotors based on TICT principles.[17c,d,18] A significant feature present in BASA was that, in contrast to the weak fluorescence intensities in solution, a significant increase was discovered in the solid state ($\Phi=0.15$). It appears that the mechanism is due to immobilization of the

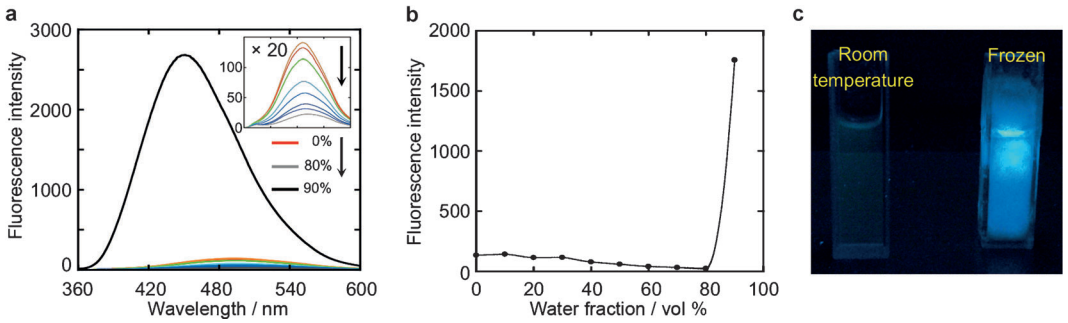

Figure 7. a) Fluorescence spectra of BASA in mixtures of DMSO–H_2O: water fraction of 0 (red), 10 (orange), 20 (yellow green), 30 (light green), 40 (light blue), 50 (cyan), 60 (blue), 70 (purple), 80 (gray), and 90% (black); b) plot of fluorescence intensity versus water volume fractions at $\lambda = 491$ nm as 0% peak maximum; and c) photographs of BASA in room temperature CH_3CN (left) and frozen (right) illuminated with a UV lamp ($\lambda = 365$ nm).

rotatable C–N bonds of amino groups. The X-ray structure of BASA revealed the existence of intramolecular distances characteristic of weaker hydrogen bonds between the side amino groups and sulfonyl groups (Figure 6a), whereas parameters for hydrogen bonds were particularly strengthened for the central aniline unit. Both adjacent amino groups were observed to adopt sp^3-like hybridization (mean plane (C1, H1, H1A)···N1 = 0.173(10) Å), whereas the central amino group was completely in an sp^2 configuration (mean plane (C7, H2, H2A)···N2 = 0.000(0) Å; Figure 6b). Additionally, the C1–N1 distance of 1.375(2) Å was longer than the C7–C2 distance of 0.351(2) Å. These structural properties together indicated that the hydrogen bonds on the adjacent amino moieties were inadequate for conjugation of an amide bond and resulted in rotation in solution. Two sulfonyl groups on both sides are hence definitely required to immobilize the amino groups.

The crystal packing of BASA revealed a dimeric structure formed through interaction between the end aniline units (Figure 6c); however, the dimeric aniline units were in a parallel form similar to an H dimer; the closest distance between carbon atoms was 3.34(3) Å, which corresponded to a higher energy state than the monomeric form in the nonemissive state.[7b,19] These results reflect that the solid-state absorption and emission of BASA showed a blueshift with respect to that found in solution. In further progress toward applying the turn-on principle to BASA, we achieved fluorescence recoveries under aggregation (AIE) in a mixture of DMSO–H_2O (Figure 7a and b) and in frozen acetonitrile (Figure 7c).[6a,18a,c,d] Both frozen and aggregation emission wavelengths were similar to those of solid-state emissions.

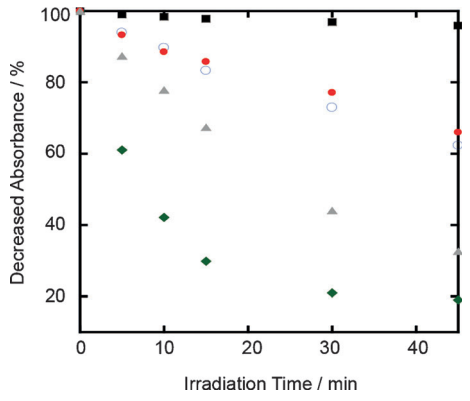

Figure 8. Plot of decreased absorbance percentage versus irradiation time for **4b** (blue, open circle), BPSA (red, filled circle), BASA (black, square), 1,8-ANS (green, rhombus), and a coumarin derivative (gray, triangle) obtained by using a 150 W xenon lamp in CH_3CN. 1,8-ANS: 8-anilino-1-naphthalenesulfonic acid ammonium salt; coumarin derivative: 7-diethylamino-4-methylcoumarin.

Photostability of BArSAs

We demonstrated the photostability of BArSAs in solution (Figure 8 and Figure S47 in the Supporting Information). The sulfonyl-bridged BPSA was slightly more stable than sulfur-bridged **4b**; this indicated that immobilization of the rotatable amino moiety exerted an effect on the hydrogen bonds. All BArSAs showed higher stability than that of ordinary fluorescent dyes,[11,20,21] such as 1,8-ANS and 7-diethylamino-4-methylcoumarin. Notably, the environmental turn-on probe BASA showed the highest stability of all dyes studied herein. In particular, BASA showed higher stability than that of 1,8-ANS; a fluorescent molecule commonly used as a polarity-sensitive probe.[22] The high stability of BASA allowed for the convenient long-term storage of a stock solution in DMSO (more than four weeks; see below).

Cell imaging

Amide-based molecules, such as Netropsin, Distamycin, and pyrrole–imidazole (Py–Im) polyamides, have an affinity for DNA.[23] BASA has similar resonance forms between the arylsulfonyl moiety and the peptide bond. To demonstrate the utility of the fluorescent properties of BASA with respect to bioimaging applications, we examined the use of BASA for the cell imaging of bovine oocyte cells arrested at the metaphase II (MII) stage, with two DNA fragments present in the cells. Confocal images of the MII oocyte cell stained with BASA clearly revealed two fragments (Figure 9a and b). In particular, dot images that characterized the chromosomes at the MII stage were observed (Figure 9a, inset). Similar images were observed when Hoechst 33342, which is a common nuclear stain, was used (Figure 9c and d). These results indicate that BASA un-

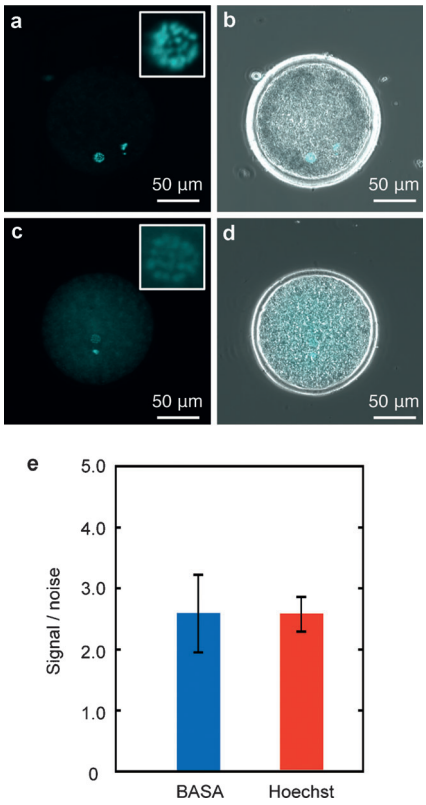

Figure 9. Imaging of bovine oocyte cells (MII stage) by BASA (200 μM; upper) and Hoechst 33342 (10 μM; lower). Excitation wavelength: 405 nm, emission filter: 420–520 nm. Best images obtained by confocal fluorescence microscopy (a and c), and superposed confocal and phase contrast microscopy (b and d). e) Plot of signal-to-noise ratio of BASA and Hoechst 33342 (mean and standard error for $n=25$ independent experiments). Insets in a) and c): Dot image characterization of the chromosomes at the MII stage.

doubtedly behaves as a DNA-selective probe. In general, cell-imaging contrast agents under short-wave UV excitation are likely to be comparatively small owing to intrinsic fluorescence and cell damage. Nevertheless, the 25 cell samples stained with BASA were well contrasted and, in some cases, were superior to Hoechst's high-contrast images (Figure 9e).

Conclusion

We have demonstrated the use of BArSAs as a novel fluorescent architecture. The most important feature of this system is that the free amino group, when not immobilized, is effectively utilized as a strong electron donor; a push–pull effect is observed in concert with sulfonyl groups functioning as electron-withdrawing groups within the fluorescent architecture. BPSA and BNSA showed efficient fluorescence and good photostability in both solution and solid state. Particularly, BASA, with amino groups on the pendant phenyl rings, imparted a high degree of fluorescence sensitivity toward polarity and viscosity; furthermore, amino group addition afforded a turn-on phenomenon in the solid state, frozen solution, and aggregation. Finally, BASA exhibited extremely high fluorescence stability and behaved as a DNA-selective probe with high contrast based on AIE. Considering the simplicity of preparation, we believe that various other BArSAs can be prepared from easily available starting materials. This strategy, which is a significant departure from conventional flat and rigid molecular design, may provide a means to construct a wide variety of solid-state fluorescent materials and bioimaging probes.

Experimental Section

General methods

All chemicals and solvents employed were of reagent grade unless otherwise indicated. Ethanol was purified by a standard distillation procedure by employing magnesium turnings and iodine prior to use. THF was purified by a standard distillation procedure with $LiAlH_4$ prior to use. All reactions were performed in standard, dry glassware under an inert atmosphere of nitrogen (N_2). Column chromatography was performed by using Kanto silica gel 60 N (spherical neutral, 40–100 μm) and Fuji Silysia Chemical NH silica gel (100–200 mesh). TLC was performed by using precoated aluminum sheets covered with 0.20 mm silica gel with fluorescent indicator ($\lambda=254$ nm) and Fuji Silysia Chemical NH TLC plates. Melting points were determined with a Yanaco MP-500P apparatus. NMR spectra were obtained on a JEOL JNM-ECX spectrometer operating at 500 MHz for ^1H or 125 MHz for ^{13}C in deuterated chloroform or deuterated DMSO with tetramethylsilane (TMS) as an internal reference (35 °C); chemical shifts (δ) are reported in ppm. Elemental analysis was obtained by using a PerkinElmer CHNS/O 2400II analyzer. IR spectroscopy was conducted by using a Horiba FTIR FREE-XACT II FT-720 instrument on KBr (press) or NaCl (cast film). Field-desorption mass spectra (FD-HRMS) were obtained on a JEOL JMS-T100GCV instrument.

Optical spectroscopy

UV/Vis spectra were measured on a Hitachi U-2810 spectrometer. Reflection spectra were measured on a Jasco V670 instrument (with an integrating sphere system). Fluorescence spectra of solutions were measured on a Hitachi F-7000 instrument. Solid-state fluorescence spectra were obtained with a Horiba Fluoromax 4 instrument. Solid-state fluorescence quantum yields were measured with a Hamamatsu C9920-01 integral sphere system.

Synthesis

2,6-Bis(benzylsulfanyl)nitrobenzene (3a): Benzyl mercaptan (5.00 g, 40.3 mmol) was added to a solution of sodium (1.11 g, 48.3 mmol) in ethanol (70 mL) at room temperature. After 30 min of stirring at ambient temperature, compound **2** (3.71 g, 19.3 mmol) was added. The resultant mixture was brought to reflux for 5 h under N_2, cooled to ambient temperature, and the resultant precipitate was filtered. The residue was washed with ethanol (50 mL) and suspended in CH_2Cl_2 (150 mL). After filtration, the solvent was removed by evaporation to yield an orange crystalline material. The residue was purified by column chromatography on silica gel (neutral; CH_2Cl_2/*n*-hexane = 2:3) to give **3a** as orange crystals (1.86 g, 26%). M.p. 81.7–82.0 °C; IR (KBr): $\tilde{\nu}=3025$ cm^{-1} (CH); ^1H NMR (500 MHz, $CDCl_3$): $\delta=7.28$–7.10 (m, Ar-*H*), 4.07 ppm (s, -CH_2-); ^1H NMR (500 MHz, [D_6]DMSO): $\delta=7.51$–7.44 (m, 3H; phenyl), 7.29–7.23 ppm (m, 10H; phenyl), 4.28 (s, 4H; -CH_2-); ^{13}C NMR (125 MHz, $CDCl_3$): $\delta=154.5$, 136.1, 132.1, 129.9, 129.5, 129.1, 128.6, 127.6, 40.2; HRMS (FD$^+$): *m/z* calcd for $C_{20}H_{17}NO_2S_2$ [M^+]: 367.07007; found: 367.07102.

2,6-Bis(phenylsulfanyl)nitrobenzene (3b): Thiophenol (5.00 g, 45.3 mmol) was added to a solution of sodium (1.35 g, 58.9 mmol) in ethanol (60 mL) at room temperature. After 30 min of stirring at ambient temperature, compound **2** (4.26 g, 22.9 mmol) was added. The resultant mixture was brought to reflux for 21 h under N_2, cooled to ambient temperature, and the resultant precipitate was filtered. The residue was washed with ethanol (50 mL) and suspended in CH_2Cl_2 (200 mL). After filtration, the solvent was removed by evaporation to give **3b** as a yellow powder (5.92 g, 77%). M.p. 116.9–117.9 °C; IR (KBr): $\tilde{\nu}$ = 3058 cm^{-1} (CH); ^1H NMR (500 MHz, $CDCl_3$): δ = 7.50–7.48 (m, 4H; phenyl), 7.39–7.38 (m, 6H; phenyl), 7.07 (t, J = 8.0 Hz, 1H; phenyl), 6.88 ppm (d, J = 8.0 Hz, 2H; phenyl); ^{13}C NMR (125 MHz, $CDCl_3$): δ = 147.9, 135.0, 134.3, 132.2, 130.8, 129.8, 129.2, 128.3 ppm; HRMS (FD^+): *m/z* calcd for $C_{18}H_{13}NO_2S_2$ [M^+]: 339.03877; found: 339.03873.

2,6-Bis(2-naphthylsulfanyl)nitrobenzene (3c): 2-Naphthalenethiol (8.00 g, 49.9 mmol) was added to a solution of sodium (1.23 g, 54.9 mmol) in ethanol (100 mL) at room temperature. After 30 min of stirring at ambient temperature, compound **2** (4.58 g, 23.8 mmol) was added. The resultant mixture was brought to reflux for 4 h under N_2, cooled to ambient temperature, and the resultant precipitate was filtered. The residue was washed with ethanol (70 mL) and suspended in CH_2Cl_2 (200 mL). After filtration, the solvent was removed by evaporation to give **3c** as an orange powder (6.51 g, 69%). M.p. 132.5–133.9 °C; IR (KBr): $\tilde{\nu}$ = 3050 cm^{-1} (CH); ^1H NMR (500 MHz, $CDCl_3$): δ = 8.07 (d, J = 2.0 Hz, 2H; naphthyl), 7.85–7.81 (m, 6H; naphthyl), 7.55–7.51 (m, 4H; naphthyl), 7.46 (dd, J = 8.5, 2.0 Hz, 2H; naphthyl), 6.99 (t, J = 8.0 Hz, 1H; phenyl), 6.87 ppm (d, J = 8.0 Hz, 2H; phenyl); ^{13}C NMR (125 MHz, $CDCl_3$): δ = 147.9, 135.2, 134.2, 133.8, 133.2, 130.8, 130.5, 129.7, 129.5, 128.4, 127.88, 127.86, 127.3, 127.0 ppm; HRMS (FD^+): *m/z* calcd for $C_{26}H_{17}NO_2S_2$ [M^+]: 439.07007; found: 439.06917.

2,6-Bis(2-aminophenylsulfanyl)nitrobenzene (3d): 2-Aminothiophenol (8.15 g, 65.1 mmol) was added to a solution of sodium (1.65 g, 71.7 mmol) in ethanol (80 mL) at room temperature. After 30 min of stirring at ambient temperature, compound **2** (6.00 g, 31.25 mmol) was added. The resultant mixture was brought to reflux for 5 h under N_2, cooled to ambient temperature, and the resultant precipitate was filtered. The residue was washed with ethanol (50 mL) and suspended in CH_2Cl_2 (300 mL). After filtration, the solvent was removed by evaporation to give a dark-red powder. The residue was washed with diethyl ether (50 mL) to give **3d** as orange crystals (4.96 g, 43%). M.p. 199.7–200.3 °C; IR (KBr): $\tilde{\nu}$ = 3473 (NH), 3367 (NH), 3054 cm^{-1} (CH); ^1H NMR (500 MHz, $CDCl_3$): δ = 7.43 (d, J = 8.0 Hz, 2H; phenyl), 7.28–7.26 (m, 2H; phenyl), 7.00 (t, J = 8.0 Hz, 1H; phenyl), 6.79–6.75 (m, 4H; phenyl), 6.64 (d, J = 8.0 Hz, 2H; phenyl), 4.28 ppm (br s, 4H; -NH_2); ^{13}C NMR (125 MHz, $CDCl_3$): δ = 149.2, 145.3, 137.9, 135.8, 132.2, 131.3, 124.7, 119.1, 115.7, 112.7 ppm; HRMS (FD^+): *m/z* calcd for $C_{18}H_{15}N_3O_2S_2$ [M^+]: 369.06057; found: 369.06161.

2,6-Bis(benzylsulfanyl)aniline (4a): 10 wt% Pd/C (250 mg) was added to a solution of **3a** (0.55 g, 1.50 mmol) in THF (30 mL) and ethanol (30 mL) under N_2. The reaction mixture was continuously shaken under a hydrogen atmosphere (balloon pressure) for 24 h. The black suspension was filtered and washed with CH_2Cl_2 (150 mL); the solvent was then removed under reduced pressure to give **4a** as a colorless oil (0.50 g, 98%). IR (NaCl): $\tilde{\nu}$ = 3444 (NH), 3345 (NH), 3058 cm^{-1} (CH); ^1H NMR (500 MHz, $CDCl_3$): δ = 7.25–7.20 (m, 7H; phenyl), 7.14–7.11 (m, 5H; phenyl), 6.44 (t, J = 7.5 Hz, 1H; phenyl), 4.96 (br s, 2H; -NH_2), 3.88 ppm (s, 4H; -CH_2-); ^{13}C NMR (125 MHz, $CDCl_3$): δ = 150.7, 138.2, 137.4, 128.9, 128.4, 127.1, 117.5, 117.3, 39.5 ppm; HRMS (FD^+): *m/z* calcd for $C_{20}H_{19}NS_2$ [M^+]: 337.09589; found: 337.09485.

2,6-Bis(phenylsulfanyl)aniline (4b): 10 wt% Pd/C (500 mg) was added to a solution of **3b** (1.00 g, 2.95 mmol) in THF (30 mL) and ethanol (30 mL) under N_2. The reaction mixture was continuously shaken under a hydrogen atmosphere (balloon pressure) for 24 h. The black suspension was filtered and washed with CH_2Cl_2 (150 mL); the solvent was then removed under reduced pressure to give **4b** as a colorless solid (0.89 g, 89%). M.p. 73.4–73.7 °C; IR (KBr): $\tilde{\nu}$ = 3469 (NH), 3363 (NH), 3056 cm^{-1} (CH); ^1H NMR (500 MHz, $CDCl_3$): δ = 7.54 (d, J = 7.5 Hz, 2H; phenyl), 7.25–7.21 (m, 4H; phenyl), 7.14–7.08 (m, 6H; phenyl), 6.73 (t, J = 7.5 Hz, 1H; phenyl), 4.98 ppm (br s, 2H; -NH_2); ^{13}C NMR (125 MHz, $CDCl_3$): δ = 152.2, 139.0, 136.0, 128.9, 126.4, 125.5, 117.8, 114.8 ppm; HRMS (FD^+): *m/z* calcd for $C_{18}H_{15}NS_2$ [M^+]: 309.06459; found: 309.06436; elemental analysis calcd (%) for $C_{18}H_{15}NS_2$: C 69.87, H 4.89, N 4.53, S 20.72; found: C 69.73, H 4.89, N 4.40, S 20.74.

2,6-Bis(2-naphthylsulfanyl)aniline (4c): 10 wt% Pd/C (800 mg) was added to a solution of **3c** (1.30 g, 2.96 mmol) in THF (40 mL) and ethanol (35 mL) under N_2. The reaction mixture was continuously shaken under a hydrogen atmosphere (balloon pressure) for 24 h. The black suspension was filtered and washed with CH_2Cl_2 (150 mL); the solvent was then removed under reduced pressure. The crude product (1.41 g) was purified by column chromatography on silica gel (NH silica gel; CH_2Cl_2) to give **4c** as colorless crystals (1.10 g, 91%). M.p. 158.7–159.2 °C; IR (KBr): $\tilde{\nu}$ = 3436 (NH), 3340 (NH), 3050 cm^{-1} (CH); ^1H NMR (500 MHz, $CDCl_3$): δ = 7.74 (dd, J = 8.0, 2.0 Hz, 2H; naphthyl), 7.70 (d, J = 8.0 Hz, 2H; phenyl), 7.62 (m, 4H; naphthyl), 7.49 (d, J = 2.0 Hz, 2H; naphthyl), 7.43–7.37 (m, 4H; naphthyl), 7.26–7.24 (m, 2H; Ar-*H*), 6.80 (t, J = 8.0 Hz, 1H; phenyl), 5.04 ppm (br s, 2H; -NH_2); ^{13}C NMR (125 MHz, $CDCl_3$): δ = 150.7, 139.1, 133.6, 133.4, 131.6, 128.6, 127.6, 126.9, 126.5, 125.5, 125.1, 124.6, 118.0, 115.1; HRMS (FD^+): *m/z* calcd for $C_{26}H_{19}NS_2$ [M^+]; 409.09589; found: 409.09431.

2,6-Bis(2-aminophenylsulfanyl)aniline (4d): 10 wt% Pd/C (250 mg) was added to a solution of **3d** (0.500 g, 1.35 mmol) in ethyl acetate (50 mL) under N_2. The reaction mixture was continuously shaken under a hydrogen atmosphere (balloon pressure) for 24 h. The black suspension was filtered and washed with CH_2Cl_2 (150 mL); the solvent was then removed under reduced pressure to give **4d** as colorless crystals (0.46 g, quant). M.p. 132.8–133.2 °C; IR (KBr): $\tilde{\nu}$ = 3457 (NH), 3357 (NH), 3050 cm^{-1} (CH); ^1H NMR (500 MHz, $CDCl_3$): δ = 7.20 (dd, J = 8.5, 1.5 Hz, 2H; phenyl), 7.12–7.09 (m, 4H; phenyl), 6.72–6.66 (m, 4H; phenyl), 6.58 (t, J = 7.5 Hz, 1H; phenyl), 4.81 (br s, 2H; -NH_2), 4.17 ppm (br s, 4H; -NH_2); ^{13}C NMR (125 MHz, $CDCl_3$): δ = 145.9, 145.3, 132.8, 131.6, 128.6, 118.1, 117.7, 117.1, 115.6, 114.6 ppm; HRMS (FD^+): *m/z* calcd for $C_{18}H_{17}N_3S_2$ [M^+]: 339.08639; found: 339.08631.

2,6-Bis(2-benzylsulfonyl)aniline (BBSA): *m*-CPBA (1.61 g, 65%, 6.07 mmol) was added to a cooled solution (0 °C) of **4a** (0.50 g, 1.48 mmol) in CH_2Cl_2 (60 mL), and the resulting suspension was stirred for 24 h at 0 °C. The reaction was quenched with a saturated aqueous solution of Na_2SO_3 (5 mL), diluted with 3 M NaOH (10 mL), and the aqueous layer was extracted with CH_2Cl_2 (2×50 mL). The combined organic layers were washed with water (3×100 mL) and brine (50 mL). After drying over anhydrous Na_2SO_4, the solvent was removed under reduced pressure to give BBSA as colorless crystals (0.511 g, 86%). M.p. 153.3–153.8 °C; IR (KBr): $\tilde{\nu}$ = 3455 (NH), 3359 (NH), 3021 (CH), 1455 (SO_2), 1122 cm^{-1} (SO_2); ^1H NMR (500 MHz, $CDCl_3$): δ = 7.55 (d, J = 8.0 Hz, 2H; phenyl), 7.33 (m, 2H; phenyl), 7.29–7.26 (m, 2H; phenyl), 7.09 (dd, J = 7.5, 1.4 Hz, 2H; phenyl),

6.56 (t, $J=8.0$ Hz, 1H; phenyl), 6.40 (br s, 2H; -NH_2), 4.32 ppm (s, 4H; -CH_2-); ^{13}C NMR (125 MHz, $CDCl_3$): $\delta=146.6$, 137.9, 130.8, 129.2, 128.8, 127.4, 120.9, 115.7, 61.2; HRMS (FD$^+$): *m/z* calcd for $C_{20}H_{19}NO_4S_2$ [M^+]: 401.07555; found: 401.07461; elemental analysis calcd (%) for $C_{20}H_{19}NO_4S_2$: C 59.83, H 4.77, N 3.49, S 15.97; found: C 59.91, H 4.77, N 3.43, S 16.08.

2,6-Bis(phenylsulfonyl)aniline (BPSA): *m*-CPBA (2.68 g, 65%, 10.87 mmol) was added to a cooled solution (0 °C) of **4b** (0.82 g, 2.65 mmol) in CH_2Cl_2 (60 mL), and the resulting suspension was stirred for 24 h at 0 °C. The reaction was quenched with a saturated aqueous solution of Na_2SO_3 (10 mL), diluted with 3 M NaOH (10 mL), and the aqueous layer was extracted with CH_2Cl_2 (2× 50 mL). The combined organic layers were washed with water (2× 100 mL) and brine (50 mL). After drying over anhydrous Na_2SO_4, the solvent was removed under reduced pressure to give BPSA as colorless crystals (0.90 g, 92%). M.p. 160.2–161.2 °C; IR (KBr): $\tilde{\nu}=$ 3471 (NH), 3367 (NH), 3072 (CH), 1457 (SO_2), 1143 cm^{-1} (SO_2); ^{1}H NMR (500 MHz, $CDCl_3$): $\delta=8.05$ (d, $J=8.0$ Hz, 2H; phenyl), 7.86–7.84 (m, 2H; phenyl), 7.61–7.58 (m, 2H; phenyl), 7.51–7.47 (m, 4H; phenyl), 6.84 (t, $J=8.0$ Hz, 1H; phenyl), 6.77 ppm (br s, 2H; -NH_2); ^{13}C NMR (125 MHz, $CDCl_3$): $\delta=145.2$, 140.8, 136.6, 133.7, 129.3, 126.9, 124.4, 116.4 ppm; HRMS (FD$^+$): *m/z* calcd for $C_{18}H_{15}NO_4S_2$ [M^+]: 373.04425; found: 373.04456; elemental analysis calcd (%) for $C_{18}H_{15}NO_4S_2$: C 57.89, H 4.05, N 3.75, S 17.17; found: C 57.86, H 3.90, N 3.64, S 17.04.

2,6-Bis(2-naphthylsulfonyl)aniline (BNSA): *m*-CPBA (1.78 g, 65%, 7.21 mmol) was added to a cooled solution (0 °C) of **4c** (0.72 g, 1.76 mmol) in CH_2Cl_2 (60 mL), and the resulting suspension was stirred for 24 h at 0 °C. The reaction was quenched with a saturated aqueous solution of Na_2SO_3 (5 mL), diluted with 3 M NaOH (10 mL), and the aqueous layer was extracted with CH_2Cl_2 (2×100 mL). The combined organic layers were washed with water (3×150 mL) and brine (100 mL). After drying over anhydrous Na_2SO_4, the solvent was removed under reduced pressure to give a dark-yellow powder (0.82 g). The crude product was purified by column chromatography on silica gel (NH silica gel; CH_2Cl_2) to give BNSA as a pale-yellow powder (0.80 g, 96%). M.p. 177.5–178.4 °C; IR (KBr): $\tilde{\nu}=3465$ (NH), 3353 (NH), 3046 (CH), 1455 (SO_2), 1126 cm^{-1} (SO_2), ^{1}H NMR (500 MHz, $CDCl_3$): $\delta=8.45$ (d, $J=1.5$ Hz, 2H; naphthyl), 8.10 (d, $J=8.0$ Hz, 2H; phenyl), 7.91 (d, $J=8.0$ Hz, 2H; naphthyl), 7.86–7.84 (m, 4H; naphthyl), 7.72 (dd, $J=9.0$, 1.5 Hz, 2H; naphthyl), 7.66–7.56 (m, 4H; naphthyl), 6.89–6.85 ppm (m, 3H; -NH_2, phenyl); ^{13}C NMR (125 MHz, $CDCl_3$): $\delta=145.4$, 137.7, 136.7, 135.3, 132.0, 129.8, 129.5, 129.4, 128.4, 128.0, 127.8, 124.6, 121.8, 116.5 ppm; HRMS (FD$^+$): *m/z* calcd for $C_{26}H_{19}NO_4S_2$ [M^+]: 473.07555; found: 473.07707; elemental analysis calcd (%) for $C_{26}H_{19}NO_4S_2$: C 65.94, H 4.04, N 2.96, S 13.54; found: C 65.85, H 4.05, N 2.84, S 13.64.

2,6-Bis(2-aminophenylsulfonyl)aniline (BASA): *m*-CPBA (3.89 g, 65%, 15.7 mmol) was added to a cooled solution (0 °C) of **4d** (1.30 g, 3.83 mmol) in CH_2Cl_2 (120 mL), and the resulting suspension was stirred for 24 h at 0 °C. The reaction was quenched with a saturated aqueous solution of Na_2SO_3 (20 mL), diluted with 3 M NaOH (30 mL), and the aqueous layer was extracted with CH_2Cl_2 (3×100 mL). The combined organic layers were washed with water (3×100 mL) and brine (100 mL). After drying over anhydrous Na_2SO_4, the solvent was removed under reduced pressure to give a pale-gray powder (1.40 g). The crude product was purified by chromatography over silica gel (NH silica gel; CH_2Cl_2/AcOEt = 4:1) and then recrystallized from CH_2Cl_2/*n*-hexane to give BASA as colorless crystals (1.20 g, 78%). M.p. 160.5–161.5 °C; IR (KBr): $\tilde{\nu}=3488$ (NH), 3465 (NH), 3390 (NH), 3372 (NH), 3064 (CH), 1485 (SO_2), 1462 (SO_2), 1132 cm^{-1} (SO_2); ^{1}H NMR (500 MHz, $CDCl_3$): $\delta=7.96$ (d, $J=$ 7.5 Hz, 2H; phenyl), 7.66 (dd, $J=8.5$, 1.0 Hz, 2H; phenyl), 7.32–7.26 (m, 2H; phenyl), 6.79–6.75 (m, 3H; phenyl), 6.67–6.61 (m, 4H; phenyl, -NH_2), 4.99 ppm (br s, 4H; -NH_2); ^{13}C NMR (125 MHz, $CDCl_3$): $\delta=146.0$, 144.8, 135.4, 135.3, 129.5, 124.3, 121.0, 118.0, 117.9, 115.3 ppm; HRMS (FD$^+$): *m/z* calcd for $C_{18}H_{17}N_3O_4S_2$ [M^+]: 403.06605; found: 403.06615; elemental analysis calcd (%) for $C_{18}H_{17}N_3O_4S_2$: C 53.58, H 4.25, N 10.41, S 15.89; found: C 53.58, H 4.19, N 10.39, S 15.87.

X-ray crystallography

Details of the structures and their refinement are summarized in the Supporting Information. CCDC 951159 (**4b**), 951160 (BBSA), 951161 (BPSA), 951162 (BNSA), and 951163 (BASA) contain the supplementary crystallographic data for this paper. These data can be obtained free of charge from The Cambridge Crystallographic Data Centre via www.ccdc.cam.ac.uk/data_request/cif..

Preparation of powder samples

Powder samples for reflection spectra, fluorescence spectra, and quantum yield measurements were obtained by grinding single crystals; all powder XRD profiles obtained were the same as simulations of 2D diffraction patterns from the corresponding single-crystal data (Figure S43 in the Supporting Information).

Fluorescence spectra of BASA in a viscous environment and AIE state

Fluorescence spectra of BASA in a viscous environment were measured in a mixture of various compositions of CH_3CN–PEG1000 (1.0×10^{-5} M). The viscosity of each solution was measured by using an A&D SV-10 Vibro viscometer instrument and the density was measured to calculate the kinematic viscosity. Fluorescence spectra for the AIE state of BASA were measured in mixtures of various compositions of DMSO–water (2.5×10^{-4} M).

Photostability determination[21a]

Photostabilities of **4b**, BPSA, BASA, 1,8-ANS, and 7-diethylamino-4-methylcoumarin were investigated by using a 150 W xenon lamp to obtain absorption spectra. UV/Vis spectra of compounds were measured after alignment in acetonitrile (5.0×10^{-5} M, $t=0$ min), followed by irradiation for 45 min. Absorption spectra were measured at regular time intervals ($t=5$, 10, 15, 30, 45 min). The measurement cell was separated from the light source at 10 cm and a clear cuvette with water was situated midway to avoid increases in temperature.

Collection of bovine cumulus oocyte complexes (COCs)

Bovine offal ovaries were collected at a local slaughterhouse and transported to the laboratory in a thermos flask at approximately 20 °C. COCs were then aspirated from visible follicles (2–8 mm in diameter). After three washes, about 20 COCs each were cultured for 22–23 h in droplets (200 μL) of a maturation medium consisting of TCM199 supplemented with 10% fetal calf serum (FCS), 0.1 IU mL^{-1} follicle-stimulating hormone (FSH), 100 units mL^{-1} penicillin G potassium (Meiji, Tokyo, Japan), and 100 μg mL^{-1} streptomycin sulfate (Meiji, Tokyo, Japan) in a humidified atmosphere of 5% CO_2 in air at 38.5 °C under a layer of mineral oil. All chemicals were purchased from Sigma–Aldrich (St. Louis, MO, USA), except for

those specifically described. The tissues and cells derived from animals used in this study were treated under the Guiding Principles for the Care and Use of Research Animals established by Yamagata University.

Observation of bovine oocyte stained by BASA

After culturing for in vitro maturation, the oocytes were denuded of cumulus cells in a phosphate-buffered saline (PBS) containing 1 mg mL^{-1} polyvinyl alcohol and 1 mg mL^{-1} hyaluronidase by using a fine-bore pipette. The cumulus-free oocytes were fixed in a paraformaldehyde solution (4% w/v in PBS) for more than 1 day. After three washes, the fixed oocytes were stained with 10 μg mL^{-1} Hoechst 33342 in PBS or 200 μg mL^{-1} BASA in DMSO/PBS (3/7, v/v) and incubated in darkness at room temperature for 30 or 120 min, respectively. The stained oocytes were examined by confocal laser-scanning microscopy (Olympus, FV10i; excitation wavelength, 405 nm; emission filter, 420–520 nm).

Acknowledgements

We thank Prof. A. Masuhara (Yamagata University) for the opportunity to use and for technical support on the Jasco V-670 UV/Vis/NIR spectrophotometer. This study was supported by the Grant-in-Aid for Young Scientist (B) (19750104 to H.K.) from the Ministry of Education, Culture, Sports, Science and Technology (MEXT) and the Foundation for Japanese Chemical Research (400(R) to H.K.).

Keywords: aggregation · biological activity · fluorescent probes · hydrogen bonds · pi interactions

[1] B. Valeur, *Molecular Fluorescence: Principles and Application*, Wiley-VCH, Weinheim, **2001**.
[2] B. Valeur, *Molecular Fluorescence: Principles and Application*, Wiley-VCH, Weinheim, **2012**.
[3] K. Müllen, U. Scherf, *Organic Light Emitting Devices, Synthesis Properties and Applications*, Wiley-VCH, Weinheim, **2005**.
[4] a) M. D. McGehee, A. J. Heeger, *Adv. Mater.* **2000**, *12*, 1655 – 1668; b) Y. Taniguchi, *J. Photopolym. Sci. Technol.* **2002**, *15*, 183 – 184.
[5] I. D. W. Samuel, G. A. Turnbull, *Chem. Rev.* **2007**, *107*, 1272 – 1295.
[6] a) Y. Hong, J. W. Y. Lam, B. Z. Tang, *Chem. Soc. Rev.* **2011**, *40*, 5361 – 5388; b) Y. Hong, J. W. Y. Lam, B. Z. Tang, *Chem. Commun.* **2009**, 4332 – 4353; c) R. Deans, J. Kim, M. R. Machacek, T. M. Swager, *J. Am. Chem. Soc.* **2000**, *122*, 8565 – 8566; d) B.-K. An, S.-K. Kwon, S.-D. Jung, S. Y. Park, *J. Am. Chem. Soc.* **2002**, *124*, 14410 – 14415; e) Q. Zeng, Z. Li, Y. Dong, C. Di, A. Qin, Y. Hong, L. Ji, Z. Zhu, C. K. W. Jim, G. Yu, Q. Li, Z. Li, Y. Liu, J. Qin, B. Z. Tang, *Chem. Commun.* **2007**, 70 – 72.
[7] a) O. Valdes-Aguilera, D. C. Neckers, *Acc. Chem. Res.* **1989**, *22*, 171 – 177; b) A. Mishra, R. K. Behera, P. K. Behera, B. K. Mishra, G. B. Behera, *Chem. Rev.* **2000**, *100*, 1973 – 2011; c) A. Loudet, K. Burgess, *Chem. Rev.* **2007**, *107*, 4891 – 4932.
[8] M. Shimizu, T. Hiyama, *Chem. Asian J.* **2010**, *5*, 1516 – 1531.
[9] a) D. Ryu, E. Park, D.-S. Kim, S. Yan, J. Y. Lee, B.-Y. Chang, K. Y. Ahn, *J. Am. Chem. Soc.* **2008**, *130*, 2394 – 2395; b) M. Wang, G. Zhang, D. Zhang, D. Zhu, B. Z. Tang, *J. Mater. Chem.* **2010**, *20*, 1858 – 1867; c) N. B. Shustova, B. D. McCarthy, M. Dincă, *J. Am. Chem. Soc.* **2011**, *133*, 20126 – 20129; d) J. Wang, J. Mei, R. Hu, J. Z. Sun, A. Qin, B. Z. Tang, *J. Am. Chem. Soc.* **2012**, *134*, 9956 – 9966.
[10] For recent examples of bioimaging based on AIE, see: a) D. Ding, K. Li, B. Liu, B. Z. Tang, *Acc. Chem. Res.* **2013**, *46*, 2441 – 2453; b) H. Shi, J. Liu, J. Geng, B. Z. Tang, B. Liu, *J. Am. Chem. Soc.* **2012**, *134*, 9569 – 9572.
[11] a) K. Kolmakov, V. N. Belov, C. A. Wurm, B. Harke, M. Leutenegger, C. Eggeling, S. W. Hell, *Eur. J. Org. Chem.* **2010**, 3593 – 3610; b) K. Kolmakov, C. Wurm, M. V. Sendev, M. L. Bossi, V. N. Belov, S. W. Hell, *Photochem. Photobiol. Sci.* **2012**, *11*, 522 – 532.
[12] R. Gompper, H.-U. Wagner, *Angew. Chem.* **1988**, *100*, 1492 – 1511; *Angew. Chem. Int. Ed. Engl.* **1988**, *27*, 1437 – 1455.
[13] Absorbance and fluorescent spectra of **4b** and BArSAs in various solvents and in the solid state (see Figures S44–46 in the Supporting Information).
[14] For an example of a flexible π-conjugation system, see: a) T. Kajiwara, K. Katagiri, M. Hasegawa, A. Ishii, M. Ferbinteanu, S. Takaishi, T. Ito, M. Yamashita, N. Iki, *Inorg. Chem.* **2006**, *45*, 4880 – 4882; b) P. Chen, R. A. Lalancette, F. Jäkle, *J. Am. Chem. Soc.* **2011**, *133*, 8802 – 8805.
[15] E. E. Jelley, *Nature* **1936**, *138*, 1009 – 1010.
[16] Z. R. Grabowski, K. Rotkiewicz, W. Rettig, *Chem. Rev.* **2003**, *103*, 3899 – 4031.
[17] a) A. Jacobson, A. Petric, D. Hogenkamp, A. Sinur, J. R. Barrio, *J. Am. Chem. Soc.* **1996**, *118*, 5572 – 5579; b) J. Zhou, X. Yuan, M. Jiang, Y. Zhang, *Macromol. Rapid Commun.* **2000**, *21*, 579 – 582; c) M. A. Haidekker, T. P. Brady, D. Lichlyter, E. A. Theodorakis, *Bioorg. Chem.* **2005**, *33*, 415 – 425; d) F. Zhou, J. Shao, Y. Yang, J. Zhao, H. Guo, X. Li, S. Ji, Z. Zhang, *Eur. J. Org. Chem.* **2011**, 4773 – 4787.
[18] a) K. A. Willets, S. Y. Nishimura, P. J. Schuck, R. J. Twieg, W. E. Moerner, *Acc. Chem. Res.* **2005**, *38*, 549 – 556; b) M. A. Haidekker, E. A. Theodorakis, *Org. Biomol. Chem.* **2007**, *5*, 1669 – 1678; c) K. A. Willets, O. Ostroverkhova, M. He, R. J. Twieg, W. E. Moerner, *J. Am. Chem. Soc.* **2003**, *125*, 1174 – 1175; d) S. J. Lord, Z. Lu, H. Wang, K. A. Willets, P. J. Schuck, H. D. Lee, S. Y. Nishimura, R. J. Twieg, W. E. Moerner, *J. Phys. Chem. A* **2007**, *111*, 8934 – 8941.
[19] a) N. Kobayashi, A. B. P. Lever, *J. Am. Chem. Soc.* **1987**, *109*, 7433 – 7441; b) K. Kameyama, M. Morisue, A. Satake, Y. Kobuke, *Angew. Chem.* **2005**, *117*, 4841 – 4844; *Angew. Chem. Int. Ed.* **2005**, *44*, 4763 – 4766.
[20] C. Eggeling, J. Widengren, R. Rigler, C. A. M. Seidel, *Anal. Chem.* **1998**, *70*, 2651 – 2659.
[21] a) G. L. Silva, V. Ediz, D. Yaron, B. A. Armitage, *J. Am. Chem. Soc.* **2007**, *129*, 5710 – 5718; b) E. Arunkumar, N. Fu, B. D. Smith, *Chem. Eur. J.* **2006**, *12*, 4684 – 4690.
[22] L. Stryer, *J. Mol. Biol.* **1965**, *13*, 482 – 495.
[23] a) S. Neidle, *Nat. Prod. Rep.* **2001**, *18*, 291 – 309; b) A. Y. Chen, C. Yu, B. Gatto, L. F. Liu, *Proc. Natl. Acad. Sci. USA* **1993**, *90*, 8131 – 8135; c) T. Bando, H. Sugiyama, *Acc. Chem. Res.* **2006**, *39*, 935 – 944.

Received: December 18, 2013
Published online on January 31, 2014